JOURNAL OF PHYSICAL ORGANIC CHEMISTRY, VOL. 5, 670–682 (1992)

GUEST DYNAMICS AND CRYSTAL STRUCTURE OF THE TRI-*o*-THYMOTIDE–ACETONE CLATHRATE STUDIED BY SOLID-STATE NMR, X-RAY DIFFRACTION AND MOLECULAR MODELLING*

G. A. FACEY, C. I. RATCLIFFE, R. HYNES AND J. A. RIPMEESTER †

Steacie Institute for Molecular Sciences, National Research Council of Canada, Ottawa, Ontario, K1A OR9, Canada

The structure of the acetone complex of tri-*o*-thymotide was solved by single-crystal x-ray diffraction. The acetone molecule is situated on the twofold axis of the cage and shows no sign of unusual disorder. Solid-state ^{2}H and ^{13}C NMR were used to show that, in addition to fast methyl group rotation, there is a rotation of the acetone molecule about the carbonyl bond. The motion is best described as a twofold flip plus the temperature-dependent population of a secondary site 63 ± 10° away from the minimum energy position. Molecular modelling calculations were used to confirm the potential shape, which was remarkably sensitive to methyl group orientation. ^{2}H spin–lattice relaxation was used to derive an activation energy of 13·6 ± 0·8 kJ mol^{-1} for the twofold flips, and the secondary site was shown to be energetically less favourable by 4·4 ± 0·5 kJ mol^{-1} from the temperature dependence of the line shape. Neither motion is seen in the diffraction experiment.

INTRODUCTION

The study of guest molecules in clathrate compounds is interesting from a physical chemical point of view. Many processes involving molecular recognition or reactions in the solid state require a definition of the dynamic structure. Two fundamental questions must be addressed: what is the preferred orientation of the guest with respect to the host cavity and what is the dynamic state of the enclathrated guest? The answers to these questions can often be obtained through the use of both solid-state NMR spectroscopy and single-crystal x-ray diffraction. These techniques are very much complementary. Each technique on its own cannot address both questions. X-ray data are sensitive to long-range order and can provide a precise description of the host structure, but often cannot do so for the guest[1,2] owing to either disorder (static or dynamic) or large-scale librational motion. The atomic positions essentially are derived from time-weighted, space-averaged electron densities. Solid-state NMR, on the other hand, is sensitive to local order and in favourable cases measures very directly the rates and amplitudes of reorientational processes. Molecular modelling[3–19] represents a third approach to obtaining information on the structure and dynamics of guest–host interactions. Comparison of calculated and experimental orientation-dependent potentials for a guest in a host cavity is a very sensitive test for both the dynamic model and the potential function employed, as the energies involved are small.

Tri-*o*-thymotide (TOT) is the trilactone of *o*-thymotic acid. In solution, the molecules take on one of two possible enantiomeric propeller conformations which are in dynamic equilibrium with each other.[20–24] When recrystallized from appropriate solvents, the molecules undergo spontaneous optical resolution and form a multitude of isostructural 2:1 (host:guest) clathrate compounds in the space group $P3_121$[22,23] and inclusion compounds in other space groups.[24–27] The twofold symmetric cavities of the $P3_121$ clathrates are bordered by eight host molecules and can accommodate single organic guest molecules whose backbones do not exceed about five atoms. Like both the host molecules and the crystals, the cavities themselves are chiral and have been used to discriminate between enantiomeric guest molecules.[1,2,24,28–38] The inner walls of the cavities are lined primarily with alkyl protons, leaving no opportunity for strong hydrogen bonding between guest and host. The forces between guest and host are therefore of the Van der Waals type and are non-specific. In this study, we used solid-state NMR, single-crystal x-ray

* Issued as NRCC No. 32953

† Author for correspondence.

0894–3230/92/100670–13$11.50

Received 3 March 1992
Revised 29 May 1992

diffraction and molecular mechanics calculations to provide a detailed description of acetone as a guest molecule in its $P3_121$ TOT cage clathrate.

THEORETICAL BACKGROUND

Broad line ^{2}H NMR

^{2}H is a spin $I = 1$ nucleus having three Zeeman states whose energies are perturbed by the electric quadrupolar interaction. Each crystallographically unique deuteron has two resonances whose energy difference depends on the quadrupolar coupling constant, $\chi = (e^2qQ/h)$, and the orientation of the electric field gradient at the nuclear site with respect to the magnetic field. The electric field gradient tensor, $\mathbf{V_{ij}}$, is usually very close to being axially symmetric about the C—D bonds of organic molecules, with its largest component, $V_{zz} = eq$, parallel to the bond. For single crystals, the quadrupolar doublets can be observed directly for each crystallographically unique deuteron. In powders, however, all orientations of the C—D bonds with respect to the magnetic field are possible. This results in a powder pattern with three pairs of features given by

$$\Delta\nu_{zz} = \nu_q \tag{1}$$

$$\Delta\nu_{yy} = \tfrac{1}{2}\nu_q(1 + \eta) \tag{2}$$

$$\Delta\nu_{xx} = \tfrac{1}{2}\nu_q(1 - \eta) \tag{3}$$

where $\nu_q = 3\chi/2$ and the asymmetry parameter $\eta = (\Delta\nu_{yy} - \Delta\nu_{xx})/\Delta\nu_{zz}$, where $0 \leqslant \eta \leqslant 1$ and $\Delta\nu_{xx} \leqslant \Delta\nu_{yy} \leqslant \Delta\nu_{zz}$ [see Figure 1(A)]. When the electric field gradient tensor is axially symmetric, $\eta = 0$ and when $\eta = 1$, $\Delta\nu_{xx} = 0$ with $\Delta\nu_{yy} = \Delta\nu_{zz}$. In all cases $\Delta\nu_{xx} + \Delta\nu_{yy} = \Delta\nu_{zz}$.

The powder line shapes are sensitive to molecular motion. For molecular motions occurring at a rate comparable to that of the static quadrupolar coupling constant (10^4–10^6 Hz), the line shapes of the Fourier-transformed quadrupolar echoes become distorted. They are sensitive to both the mechanism and rate of the motion occurring. Such line shapes have been simulated and used to study molecular motions on this time scale.[39,40] For fast molecular motions (rate $\geqslant 10^7$ Hz), the situation is much simpler. The static electric field gradient tensor, $\mathbf{V_{ij}}$ can be described in a reference coordinate system defined by the Euler angles,[41] α, β and γ, thus giving $\mathbf{V}_{\alpha,\beta,\gamma} = a_{ij}$ for each of the positions visited over the course of the molecular motion. The weighted average of all of the tensor components can then be calculated yielding an average tensor, $\mathbf{V}'_{\alpha,\beta,\gamma}$, where

$$V'_{\alpha,\beta,\gamma} = \begin{matrix} a'_{11} & a'_{12} & a'_{13} \\ a'_{12} & a'_{22} & a'_{23} \\ a'_{13} & a'_{23} & a'_{33} \end{matrix} \tag{4}$$

The general definitions of the tensor components, a_{ij}, in terms of the Euler angles have been tabulated.[42] If an appropriate reference coordinate system is chosen, the averaged tensor, $\mathbf{V}'_{\alpha,\beta,\gamma}$, is diagonal and the principal components, V'_{xx}, V'_{yy} and V'_{zz}, defining the new spectral parameters, $\Delta\nu'_{xx}$, $\Delta\nu'_{yy}$ and $\Delta\nu'_{zz}$, can be obtained directly. If the appropriate reference system is not chosen, the averaged tensor must be diagonalized. The powder line shape is simulated from the calculated spectral parameters.[43,44] If more than one fast molecular motion is present, this procedure can be applied consecutively to obtain the motionally averaged powder spectrum.

Often ^{2}H NMR powder line shapes, averaged by fast molecular motion, give the mechanistic details of the motion but no quantitative details regarding the rate or activation energy barrier. One way of obtaining such information experimentally is to measure the spin–lattice relaxation time, T_1 as a function of temperature. The rate of relaxation, $R_1 = (1/T_1)$, can be described by the following equation:[45,46]

$$R_1 = KJ(\omega_0, \tau_c) \tag{5}$$

where K is a constant depending on the quadrupolar coupling constant, the type of molecular motion and the point in the powder spectrum at which the relaxation time is measured. $J(\omega_0, \tau_c)$ is a spectral density function depending on the Larmor frequency, ω_0 and the correlation time of the motion, τ_c. For specific motions with single correlation times, $J(\omega_0, \tau_c)$ can be represented by[47]

$$J(\omega_0, \tau_c) = \frac{\tau_c}{1 + (\omega_0\tau_c)^2} + \frac{4\tau_c}{1 + (2\omega_0\tau_c)} \tag{6}$$

$J(\omega_0, \tau_c)$ is a maximum when $\omega_0\tau_c = 0{\cdot}6158$. At this point, relaxation is most efficient and T_1 is a minimum. The correlation time of the motion is therefore easily found at the T_1 minimum. In the extreme narrowing limit, where $\omega_0\tau_c \ll 1$, the rate of relaxation is linear in

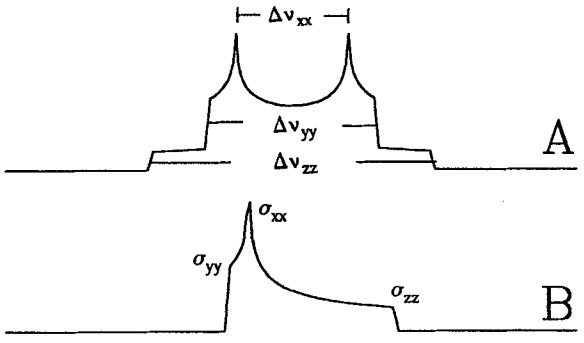

Figure 1. Sample powder spectra. (A) ^{2}H NMR powder pattern; (B) ^{13}C NMR powder spectrum. In both cases the asymmetry parameter is 0·2

τ_c. The correlation time of the motion is related to the absolute temperature by the Arrhenius relationship:

$$\tau_c = \tau_0 e^{E_a/RT} \quad (7)$$

where τ_0 is a constant, E_a is the activation energy of the motion and R is the gas constant. In the extreme narrowing limit, the activation energy can be obtained from the slope of a plot of log T_1 vs $1/T$.

When two molecular motions of different correlation times, τ_{c1} and τ_{c2}, occur simultaneously, the spectral density function depends on both correlation times.[48] If, however, one of the correlation times, τ_{c2} is of the order of $1/\omega_0$ and the other, τ_{c1} is very short such that $\omega_0\tau_c \ll 0{\cdot}6158$ and $\tau_{c1} \ll \tau_{c2}$, then the motion with correlation time, τ_{c1}, contributes very little to the relaxation and the spectral density function in equation (6) holds with $\tau_c = \tau_{c2}$.

Broad line ^{13}C NMR

Unlike ^{2}H, ^{13}C is a spin $I = \frac{1}{2}$ nucleus having only two Zeeman states. Each crystallographically unique ^{13}C nucleus can therefore have only one resonance line. The precise frequency of the resonance depends on the orientation of the chemical shielding tensor σ_{ij} with respect to the magnetic field. If the ^{1}H–^{13}C dipolar interaction is removed by high-power ^{1}H decoupling, the ^{13}C NMR spectrum of a single crystal will consist of a sharp line for each crystallographically unique ^{13}C nucleus. In powders, where all orientations of the chemical shielding tensor with respect to the magnetic field are possible, a powder pattern is obtained. The line shape is similar to that expected for only one of the two energy transitions of a deuteron and therefore the spectrum is not generally bilaterally symmetric. Instead of being characterized by three pairs of features, ^{13}C powder patterns are characterized by three single features, σ_{xx}, σ_{yy} and σ_{zz}. These are proportional to the principal components of the chemical shielding tensor and can be read directly from the powder spectrum [see Figure 1(B)].

Like the electric field gradient tensor, the chemical shielding tensor is averaged by molecular motions. When the motion is fast, relative to the full frequency spread of the rigid powder pattern, the averaged spectrum for each unique ^{13}C nucleus is the result of a single averaged tensor. The averaged parameters, σ'_{xx}, σ'_{yy} and σ'_{zz}, are obtained using the same principles as described above for averaging ^{2}H electric field gradient tensors and again the motionally narrowed spectrum can be simulated using the averaged parameters.[43,44]

Often it is difficult to obtain a powder spectrum for a ^{13}C species in a particular chemical environment due to the very low signal-to-noise ratio resulting from the signal being spread over a large frequency range and from overlap with other ^{13}C signals. It is possible to overcome this problem by obtaining one or more ^{13}C cross-polarization magic angle spinning (CP/MAS) NMR spectra at slow spinning rates. The envelope of spinning sidebands approximates the powder spectrum at slow spinning rates. A graphical method,[49] based on sideband intensities and spinning rates, can be used to obtain reliable values for σ_{xx}, σ_{yy} and σ_{zz}.

EXPERIMENTAL

Previously described methods were used to prepare *o*-thymotic acid from thymol,[50] which in turn was used to prepare tri-*o*-thymotide.[51] The crude synthetic product was recrystallized twice from acetone. The purity of this material was tested by examination of the solid-state ^{13}C CP/MAS NMR spectrum, where no impurities were detected. The TOT–acetone clathrate was heated for 48 h at 150 °C in order to remove the enclathrated acetone. A sample of this material was also examined by ^{13}C CP/MAS NMR to ensure that all of the acetone had been removed. Acetone-d_6 and [2-^{13}C]acetone were purchased from MSD. The [2-^{13}C]acetone was diluted as follows: 0·5 g of [2-^{13}C]acetone was mixed with 4·5 ml of unlabelled acetone to produce approximately 12 mol% ^{13}C-enriched acetone. The labelled clathrates were prepared by adding small amounts of guest (*ca* 5 ml) to *ca* 250 mg of desolvated TOT. The mixtures were heated to boiling. The hot mother liquor was removed and allowed to cool, forming small crystals of the desired clathrate. The cool mother liquor from this mixture was returned to the original mixture and the cycle repeated until all of the TOT had been dissolved and recrystallized. The quality of the clathrates was confirmed by solid-state ^{13}C CP/MAS NMR.

A crystal, suitable for x-ray analysis, was grown by slow recrystallization of desolvated TOT from acetone. The cell constants were determined from 25 reflections with 2θ in the range 80–100°. The intensity data were obtained at room temperature on a Nonius diffractometer using the $\theta/2\theta$ scan mode. No correction was necessary for absorption. Of the 2691 reflections measured, 1889 were unique and, of these, 1624 had intensities greater than that of the background by 2·5 standard deviations. Least-squares refinement was carried out with NRC-VAX software[52] using the 1624 reflections with weighting factors, w, based on counting statistics where $w = (1/\sigma_{Fo})^2$. The final R value was 0·023.

Solid-state ^{2}H NMR experiments were carried out at 27·6 MHz on a Bruker CXP-180 pulse NMR spectrometer using the ($\pi/2$–τ–$\pi/2$–τ–acquire) quadrupolar echo pulse sequence.[53] The delay between pulses was set at 35 μs using 3 μs $\pi/2$ pulses and repetition times of between 1 and 10 s depending on T_1. The temperature was controlled with a Bruker temperature control unit using cold nitrogen gas, a thermocouple and an electric heater. The temperatures were accurate to within ±1 K. The spectrum obtained at 77 K was

acquired while the NMR coil was fully immersed in liquid nitrogen.

^{2}H T_1 measurements were carried out for the TOT–acetone-d_6 clathrate as a function of temperature. Complete measurements were made using the inversion–recovery technique in conjunction with the quadrupolar echo pulse sequence at 298, 236 and 184 K. The intensity measurements were all made at the same point in the spectrum. The T_1s were calculated using the two parameter model:

$$I(\tau) = I_\infty(1 - 2e^{-\tau/T_1}) \quad (8)$$

where $I(\tau)$ is the intensity of the inner peaks of the spectrum as a function of the relaxation delay, τ, and I_∞ is their intensity in the fully relaxed spectrum. Other T_1 estimates were made at 298, 211, 200, 184, 175 and 162 K by finding the τ value that gave a minimum signal, τ_{null}. The T_1 value was then obtained from equation (8) by substituting $I(\tau) = 0$ and $\tau = \tau_{null}$. The T_1 estimates made at 298 and 184 K using the null method agreed well with those determined by the inversion–recovery technique.

^{13}C CP/MAS experiments used to obtain the chemical shielding parameters for the carbonyl carbon of the enclathrated ^{13}C enriched acetone were conducted at 45·3 MHz on the same spectrometer. The ^{1}H $\pi/2$ pulses were typically 4 μs. Cross-polarization times of 3 ms were used with repetition times of 2 s. Four spectra were recorded at different spinning rates. The rates were chosen to minimize the degree of overlap between the acetone carbonyl spinning sidebands and any of the resonances or spinning sidebands due to the host. The spinning rates were between 2·176 and 2·389 kHz and were stable to within a few Hz. The acetone carbonyl peak, which was the most intense in the spectrum, was normalized to unit intensity and the intensities of the sidebands were measured as a ratio to the centre band. The intensity ratios were used in a graphical sideband analysis[49] to determine the parameters of the chemical shielding tensor for the carbonyl carbon of TOT enclathrated acetone at room temperature.

Molecular mechanics calculations were carried out using the Maxmin2 force field of the SYBYL[54] software package installed on a Silicon Graphics Personal Iris computer. Coulombic terms were included with partial charges calculated using the Gasteiger–Hückel option provided in the software.

RESULTS AND DISCUSSION

Single-crystal x-ray data

The crystallographic coordinates and thermal parameters of the host and guest are given in Tables 1 and 2, respectively, with the numbering scheme of Figure 2. It was found to be a typical[5] 2:1 $P3_121$ clathrate with cell dimensions $a = b = 13·4612(11)$ Å and $c = 30·2973(20)$ Å. There are six TOT molecules in the unit cell. Each acetone molecule is inside a cage of eight TOT molecules. Its carbonyl bond is on the twofold symmetry axis of the clathrate cavity. The structure can be considered well ordered, with no obvious signs of large-scale disorder. The anisotropic thermal parameters for the methyl groups in both host and guest are larger than those for most of the other framework atoms, as expected. Other than that, the guest carbonyl carbon and oxygen, and also the host carbonyl oxygens O2 and O4, exhibit some signs of larger than usual

Table 1. X-ray coordinates for TOT–acetone

Atom	*x*	*y*	*z*
O1	0·4693(3)	0·8887(3)	0·09431(11)
O2	0·3736(4)	0·7233(3)	0·05693(12)
O3	0·3389(3)	0·8256(3)	0·17174(11)
O4	0·1696(4)	0·7000(4)	0·14217(18)
O5	0·3341(3)	0·9896(3)	0·10553(12)
O6	0·2087(4)	0·8970(4)	0·05056(14)
C1	0·4121(5)	0·7725(5)	0·09096(19)
C2	0·4116(5)	0·7170(5)	0·13379(18)
C3	0·4511(5)	0·6376(5)	0·13467(19)
C4	0·4998(5)	0·6121(5)	0·09453(18)
C5	0·4471(5)	0·5865(5)	0·17507(22)
C6	0·4047(5)	0·6115(6)	0·21249(18)
C7	0·3682(5)	0·6894(5)	0·21237(18)
C8	0·3231(6)	0·7162(6)	0·25431(18)
C9	0·2258(6)	0·6090(6)	0·27454(19)
C10	0·4193(6)	0·7785(6)	0·28826(18)
C11	0·3719(5)	0·7404(5)	0·17247(19)
C12	0·2314(6)	0·7927(6)	0·15748(21)
C13	0·2017(5)	0·8846(5)	0·16347(19)
C14	0·1274(5)	0·8745(6)	0·19763(20)
C15	0·0710(5)	0·7726(6)	0·22703(19)
C16	0·1053(6)	0·9650(7)	0·20166(19)
C17	0·1522(6)	1·0580(6)	0·17361(23)
C18	0·2245(6)	1·0674(5)	0·13905(21)
C19	0·2729(6)	1·1673(6)	0·10787(21)
C20	0·1812(6)	1·1538(6)	0·07495(20)
C21	0·3229(6)	1·2833(6)	0·13099(24)
C22	0·2492(5)	0·9794(6)	0·13531(18)
C23	0·3021(6)	0·9463(5)	0·06375(21)
C24	0·4118(5)	0·9784(5)	0·03839(18)
C25	0·4348(6)	1·0432(5)	−0·00042(18)
C26	0·3510(5)	1·0780(5)	−0·01886(17)
C27	0·5394(6)	1·0795(5)	−0·02086(18)
C28	0·6191(5)	1·0537(5)	−0·00417(19)
C29	0·5985(6)	0·9882(5)	0·03409(19)
C30	0·6853(6)	0·9611(6)	0·05291(19)
C31	0·7190(6)	0·8968(7)	0·02087(19)
C32	0·7948(6)	1·0727(6)	0·06643(22)
C33	0·4941(6)	0·9527(5)	0·05409(17)
O	0·7736(6)	0·7736	1/2
CA1	0·6873(9)	0·6873	1/2
CA2	0·5839(7)	0·6797(8)	0·4838(3)

Table 2. Thermal parameters for TOT–acetone

Atom	u11(U)	u22	u33
O1	5·9(3)	4·5(3)	3·65(24)
O2	13·5(5)	4·5(3)	4·9(3)
O3	3·8(3)	4·8(3)	4·64(24)
O4	7·9(4)	6·5(4)	23·0(6)
O5	4·6(3)	5·1(3)	4·44(23)
O6	4·9(3)	9·0(4)	7·1(3)
C1	5·7(5)	3·7(5)	5·0(4)
C2	4·2(4)	3·6(4)	4·3(4)
C3	5·7(5)	4·7(5)	6·0(5)
C4	10·1(6)	7·3(6)	7·9(4)
C5	6·5(5)	4·7(5)	7·7(5)
C6	6·4(5)	6·7(6)	5·4(4)
C7	5·0(5)	6·3(5)	4·5(4)
C8	7·0(6)	10·3(6)	4·9(4)
C9	7·1(6)	11·5(7)	6·7(5)
C10	9·9(6)	11·0(6)	5·7(4)
C11	4·2(4)	4·0(4)	5·0(4)
C12	6·2(6)	5·7(6)	6·5(5)
C13	4·4(5)	4·7(5)	5·2(4)
C14	4·7(5)	7·1(6)	5·1(4)
C15	5·7(5)	9·0(6)	6·1(4)
C16	5·3(5)	8·5(6)	5·4(4)
C17	5·1(5)	6·6(6)	7·9(5)
C18	5·0(5)	4·2(5)	6·7(5)
C19	6·4(5)	5·5(5)	9·4(6)
C20	12·6(7)	10·2(7)	8·8(5)
C21	9·6(7)	5·2(6)	14·2(8)
C22	4·4(5)	5·0(5)	4·8(4)
C23	6·4(6)	3·9(5)	5·1(5)
C24	5·1(5)	4·1(5)	3·7(4)
C25	6·7(6)	4·7(5)	4·4(4)
C26	7·7(6)	6·7(5)	7·0(4)
C27	7·9(6)	5·0(5)	4·5(4)
C28	5·5(5)	5·2(5)	4·4(5)
C29	4·9(5)	4·7(5)	4·6(4)
C30	5·3(5)	7·2(6)	5·4(5)
C31	15·3(8)	18·7(9)	7·9(5)
C32	7·8(6)	10·1(7)	12·4(7)
C33	6·5(6)	3·8(4)	3·0(4)
O	9·9(5)	9·9	32·7(13)
CA1	6·9(7)	6·9	14·0(11)
CA2	9·1(8)	18·8(12)	19·4(10)

thermal motion. Previously this has been interpreted in terms of a twofold disorder of the carbonyl oxygens.[28]

Solid-state ^{2}H NMR data

The solid-state ^{2}H NMR spectrum of the TOT–acetone-d_6 clathrate was obtained as a function of temperature. The spectra are shown in Figure 3(A). The spectrum obtained at 77 K can be well represented by a fast motional spectrum [Figure 3(B)]. Those between 77 and 156 K have distorted line shapes owing to a molecular motion occurring on the same time scale as $1/\chi$. The spectra obtained at temperatures above 156 K become narrower with increasing temperature. These spectra are in the fast motional regime and can be simulated [Figures 3(C) and (D)].

For a completely rigid acetone molecule, one expects an axially symmetric spectrum with $\Delta\nu_{xx} = \Delta\nu_{yy} \approx 126$ kHz and $\Delta\nu_{zz} \approx 252$ kHz.[55] For fast symmetric methyl group rotations, one expects the same spectrum scaled down by a factor of $\frac{1}{2}(3\cos^2\beta - 1)$ compared with that of the rigid spectrum, where β is the tetrahedral angle between the C—D bonds and the rotation axis. For such a motion, the parameters are $\Delta\nu'_{xx} = \Delta\nu'_{yy} = 42$ kHz and $\Delta\nu'_{zz} = 84$ kHz. The spectral parameters observed at 77 K were $\Delta\nu'_{xx} = 35 \pm 1$ kHz, $\Delta\nu'_{yy} = 48 \pm 2$ kHz and $\Delta\nu'_{zz} = 83 \pm 3$ kHz. These agree well with those measured for pure solid acetone-d_6 at 77 K.[56,57] The axial asymmetry observed in the spectrum is not uncommon for rotating methyl groups attached to carbonyl carbons.[56] It can be accounted for if the three sites visited by the deuterons over the course of the rotation are inequivalent. This is indeed the case for the acetone molecule. The motional narrowing in the spectrum obtained at 77 K is therefore due to fast methyl group rotation. The V'_{zz} components of the averaged electric field gradient tensors are approximately parallel to the C—C bonds in the molecule. The other components are in and out of the molecular plane, but it is not possible to assign their orientations at this stage.

Above 77 K a new molecular motion appears and reaches the fast motional regime at 156 K. Since the averaged spectrum at 156 K is a single powder pattern, i.e. it is not a superposition of two, then the motion must treat both methyl groups in exactly the same way. One such motion is a twofold flip about the carbonyl bond. This motion would be consistent with the x-ray data since the carbonyl bond was found to be coincident with the twofold axis of the cage. A discrete twofold flip about this axis does not give rise to disorder and would not be expected to show up in the x-ray data. The effects on the already averaged ^{2}H NMR spectrum at 77 K can be calculated.[42] The new averaged tensor components, V''_{xx}, V''_{yy} and V''_{zz}, are given by the following equations:

$$V''_{xx} = V'_{ii}\sin^2\beta + V'_{zz}\cos^2\beta \quad (9)$$

$$V''_{yy} = -V'_{jj} \quad (10)$$

$$V''_{zz} = V'_{ii}\cos^2\beta + V'_{zz}\sin^2\beta \quad (11)$$

where β, in this case, is the angle between the C—C and carbonyl bond axes. According to microwave data,[58,59] $\beta = 58°$. Since the orientations of the V'_{xx} and V'_{yy} components at 77 K are not known, one must consider two possible situations: either V'_{xx} is in the molecular plane and V'_{yy} is out of the molecular plane ($i = x, j = y$), or vice versa ($i = y, j = x$). Each of these situations leads

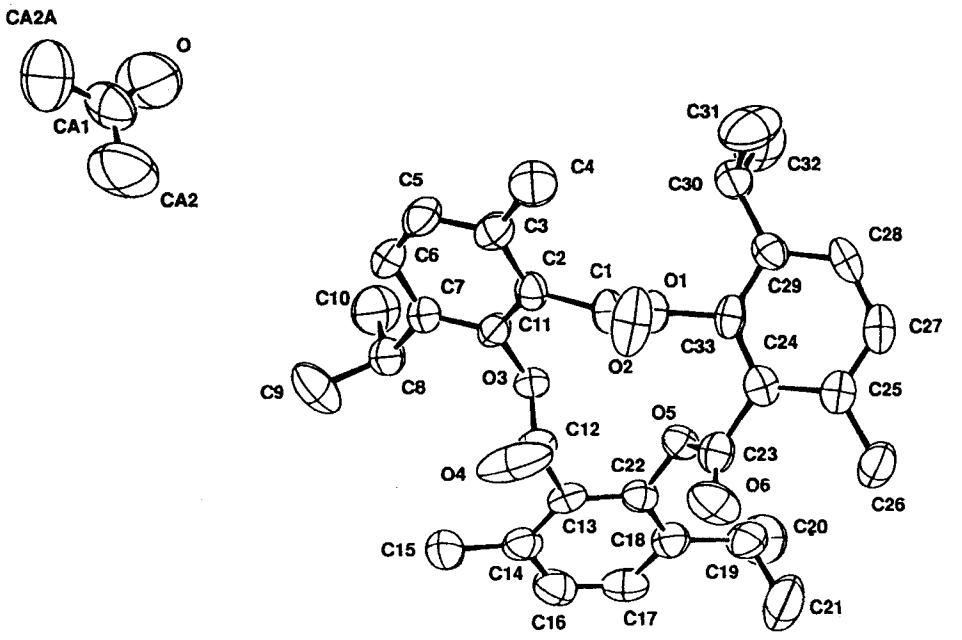

Figure 2. ORTEP diagram of the TOT–acetone clathrate showing the numbering scheme used in the presentation of the x-ray coordinates in Tables 1 and 2

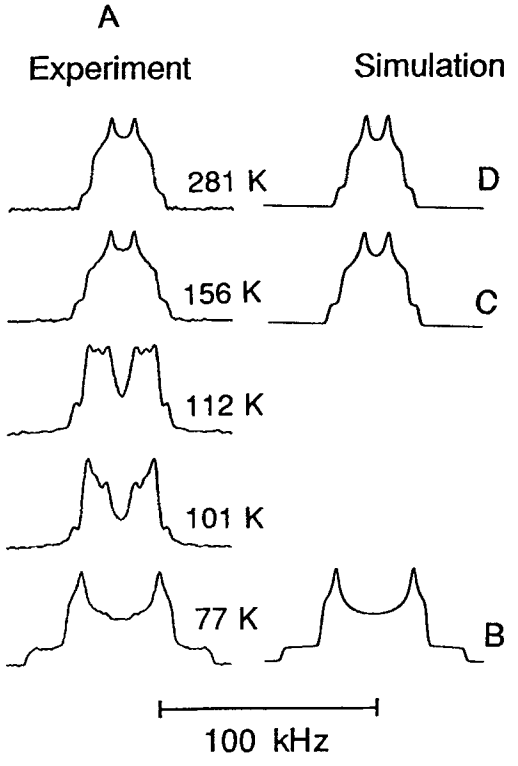

Figure 3. (A) Solid-state 27·6 MHz ^{2}H NMR spectra of TOT–acetone-d_6 as a function of temperature. The spectra were acquired using the quadrupolar echo pulse sequence. (B) Simulation of the spectrum at 77 K using the following parameters; $\langle\chi\rangle = 55{\cdot}3$ kHz, $\eta = 0{\cdot}156$, Gaussian broadening = 1·8 kHz. (C) Simulation of the spectrum at 156 K using the following parameters; $\langle\chi\rangle = 27{\cdot}3$ kHz, $\eta = 0{\cdot}463$, Gaussian broadening = 1·8 kHz. (D) Simulation of the spectrum at 281 K using the following parameters, $\langle\chi\rangle = 23{\cdot}3$ kHz, $\eta = 0{\cdot}432$, Gaussian broadening = 1·8 kHz

to a different spectrum when fast twofold flips occur. If the former is true, then the splittings in the fast motion limit spectrum are expected to be $\Delta\nu''_{xx} = 2$ kHz, $\Delta\nu''_{yy} = 48$ kHz and $\Delta\nu''_{zz} = 50$ kHz ($\eta = 0{\cdot}92$). If the latter is true, then $\Delta\nu''_{xx} = 11$ kHz, $\Delta\nu''_{yy} = 35$ kHz and $\Delta\nu''_{zz} = 46$ kHz ($\eta = 0{\cdot}52$). The parameters for the observed spectrum at 156 K were $\Delta\nu''_{xx} = 10{\cdot}4 \pm 0{\cdot}5$ kHz, $\Delta\nu''_{yy} = 32.1 \pm 1$ kHz and $\Delta\nu''_{zz} = 42{\cdot}5 \pm 1$ kHz ($\eta = 0{\cdot}51$). These parameters do not match either of the two situations exactly but are certainly closer to those of the latter than the former, suggesting that the V'_{yy} and V'_{xx} components of the electric field gradient tensor at 77 K must be in and out of the molecular plane, respectively (see Figure 4). Two of the three parameters of the spectrum undergo further averaging at higher temperatures (Figure 5). This is not expected for simple

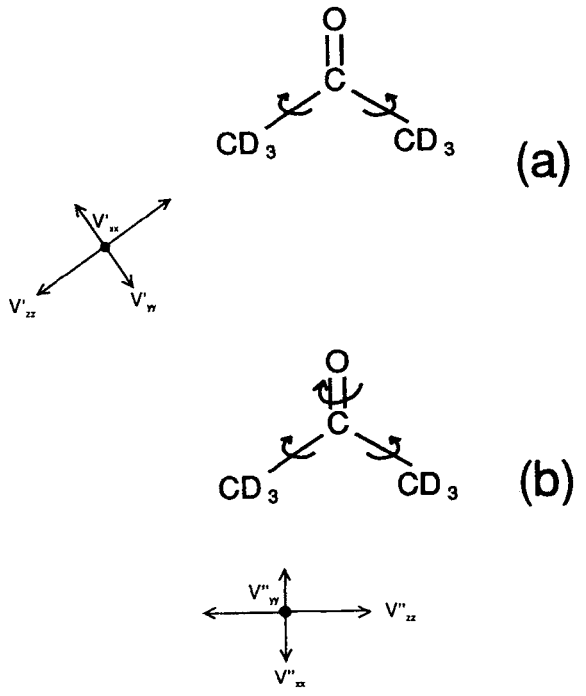

Figure 4. (A) Diagram showing the orientations of the averaged electric field gradient tensor components, V'_{xx}, V'_{yy} and V'_{zz}, resulting from fast methyl group rotation. (B) Diagram showing the orientations of the averaged electric field gradient tensor components, V''_{xx}, V''_{yy} and V''_{zz}, resulting from both fast methyl group rotation and fast twofold flips about the carbonyl bond

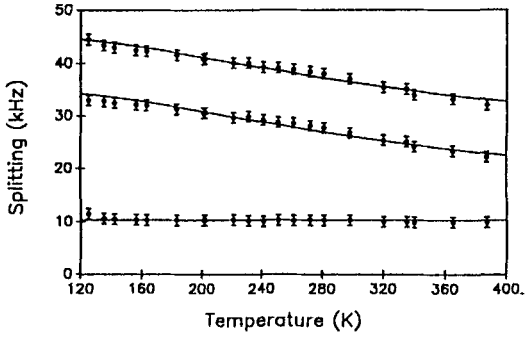

Figure 5. Plot of the frequency separation between the three sets of features in the solid-state ^2H NMR spectra of TOT–acetone-d_6 as a function of temperature. The splittings were measured directly from the spectra. The measurements made below 156 K are from intermediate rate spectra where the parameters were obvious. The lines were drawn according to the four-site model using the best fitting parameters described in the text. Notice that one of the components, $\Delta\nu''_{xx}$, is independent of temperature

twofold flips plus methyl group rotations and indicates that the motion occurring at temperatures $\geqslant 156$ K, giving rise to the spectral parameters $\Delta\nu''_{xx}$, $\Delta\nu''_{yy}$ and $\Delta\nu''_{zz}$, is more complicated than a simple twofold rotation about the carbonyl bond. Note that the averaged $\Delta\nu''_{xx}$ component for the twofold rotation is parallel to both the carbonyl bond of the guest molecule and the twofold axis of the cavity. Further, it is this component which remains unchanged above 156 K with an average value of 10·3 kHz. This suggests that whatever the more complicated motion is it must still involve reorientation about the twofold axis, thus giving rise to further averaging of only the other two components.

One possible model which takes into account both the twofold symmetry and the chirality of the clathrate cage is a four-site potential for the rotation of the acetone molecule about its carbonyl bond (see Figure 6). The sites at 0° and 180° have populations $(1 + x)$ while those at $\delta°$ and $(180° + \delta°)$ have populations $(1 - x)$. The energy difference, ΔE, between the two different types of sites is then given by the Boltzman factor:

$$\frac{(1+x)}{(1-x)} = e^{\Delta E/RT} \tag{12}$$

Using the spectral parameters at 77 K as the starting point, the averaged electric field gradient tensor can be calculated:

$$a''_{11} = \frac{(1+x)+(1-x)\cos^2\delta}{2}(\cos^2\beta V'_{yy} + \sin^2\beta V'_{zz}) + \frac{(1-x)\sin^2\delta}{2}V'_{xx} \tag{13}$$

$$a''_{22} = \frac{(1-x)\sin^2\delta}{2}(\cos^2\beta V'_{yy} + \sin^2\beta V'_{zz}) + \frac{(1-x)+(1+x)\cos^2\delta}{2}V'_{xx} \tag{14}$$

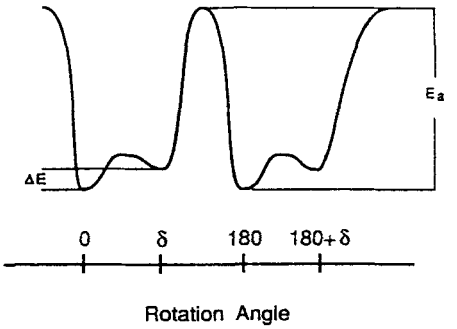

Figure 6. Representation of the four-site potential describing the rotation of the TOT-enclathrated acetone molecule about the carbonyl bond

$$a''_{33} = \sin^2 \beta V'_{yy} + \cos^2 \beta V'_{zz} \quad (15)$$

$$a''_{12} = a''_{21} = \frac{(1-x)\sin \delta \cos \delta}{2} \times [-(\cos^2 \beta V'_{yy} + \sin^2 \beta V'_{zz}) + V'_{xx}] \quad (16)$$

$$a''_{13} = a''_{31} = a''_{23} = a''_{32} = 0 \quad (17)$$

where β is the angle between the axis of rotation (the carbonyl bond) and the C—C bonds. This tensor can be diagonalized to give the spectral parameters directly:

$$V''_{xx} = \sin^2 \beta V'_{yy} + \cos^2 \beta V'_{zz} \quad (18)$$

$$V''_{yy} = (\cos^2 \beta V'_{yy} + \sin^2 \beta V'_{zz}) \frac{(1-\Omega)}{2} + V'_{xx} \frac{(1+\Omega)}{2} \quad (19)$$

$$V''_{zz} = (\cos^2 \beta V'_{yy} + \sin^2 \beta V'_{zz}) \frac{(1+\Omega)}{2} + V'_{xx} \frac{(1-\Omega)}{2} \quad (20)$$

where

$$\Omega = \sqrt{x^2 \sin^2 \delta + \cos^2 \delta} \quad (21)$$

Note that V''_{xx} and hence $\Delta\nu''_{xx}$ are independent of both x and δ and therefore independent of temperature.

When the 77 K parameters are substituted with $\beta = 57{\cdot}6^\circ$ (chosen to make V''_{xx} the same as the observed component), $V''_{xx} = -10{\cdot}3$ kHz, $V''_{yy} = (10{\cdot}3 - 80{\cdot}3\Omega)/2$ kHz and $V''_{zz} = (10{\cdot}3 + 80{\cdot}3\Omega)/2$, from which $\Omega = (V''_{zz} - V''_{yy})/80{\cdot}3$. Unfortunately, since Ω contains two unknowns, ΔE and δ, this does not give a unique solution at any one temperature. However, the whole set of data can be fitted to find the best pair of values for ΔE and δ. The best fit was obtained for $\delta = 63^\circ$ and $\Delta E = 4{\cdot}4$ kJ mol^{-1} shown in Figure 6. Considering the errors in the data, reasonably close fits can also be obtained within the limits of $\delta = 56^\circ$, $\Delta E = 4{\cdot}0$ kJ mol^{-1} at one extreme and $\delta = 75^\circ$, $\Delta E = 4{\cdot}9$ kJ mol^{-1} at the other. This leads to estimated errors of $\pm 10^\circ$ in δ and $\pm 0{\cdot}5$ kJ mol^{-1} in ΔE. The fit using this simple model is very encouraging, especially when one considers that δ and ΔE are both likely to have some temperature dependence as the potential may be affected by motions of groups in the host lattice.

The variable-temperature ^{2}H T_1 data are summarized in Table 3. The errors are estimated to be $\pm 5\%$ for the T_1s measured by using the inversion–recovery technique and $\pm 15\%$ for those estimated by using the null signals. An Arrhenius plot of the data is given in Figure 7. The first five data points on the Arrhenius plot give a straight line whose slope can be used to obtain an activation energy of $13{\cdot}6 \pm 0{\cdot}8$ kJ mol^{-1}. This barrier is much higher than that reported for the methyl group rotation in gaseous acetone-d_6 ($3{\cdot}0$ kJ mol^{-1}).[60] Because of the large difference, the activation barrier measured here must be due to the reorientation of the acetone molecule about the carbonyl bond. The T_1 minimum is 19 ± 1 ms at 184 K. If it is assumed that the correlation time of the methyl group rotation, τ_{c1}, is much shorter than that for the reorientation about the carbonyl bond, τ_{c2} then the correlation time for the molecular reorientation at the T_1 minimum (*ca* 184 K) is $3{\cdot}55$ ns.

Table 3. ^{2}H T_1s for TOT–acetone-d_6

Temperature (K)	T_1 (ms)	Method
298	603	Inversion–recovery
298	577	Null
236	92	Inversion–recovery
211	36	Null
200	25	Null
184	19.3	Inversion–recovery
184	19	Null
175	20	Null
162	29	Null

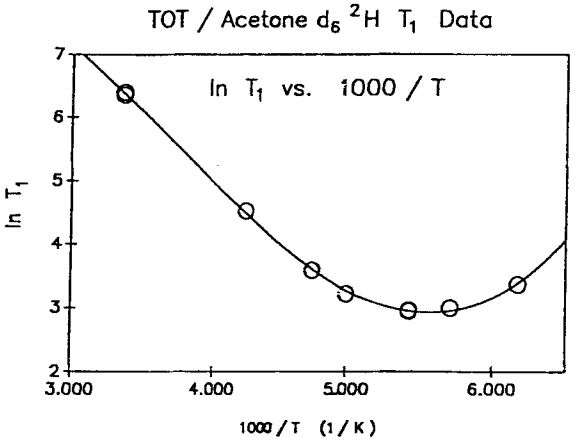

Figure 7. Arrhenius plot (ln T_1 vs 1000/T) of the T_1 data for TOT–acetone-d_6

Solid-state ^{13}C NMR data

The ^{13}C CP/MAS NMR spectrum of the TOT–acetone clathrate is shown in Figure 8. The resonances of the host appear as triplets, many of which are completely resolved. This indicates that the threefold molecular symmetry of the TOT molecule is lost in the solid clathrate. The resonances of the carbonyl carbons of the TOT host are particularly sharp and indicate that the higher than expected thermal parameters observed for the cabonyl groups in the crystal structure must be due to dynamic rather than static disorder. The resonances of the acetone guest appear at 206·6 and

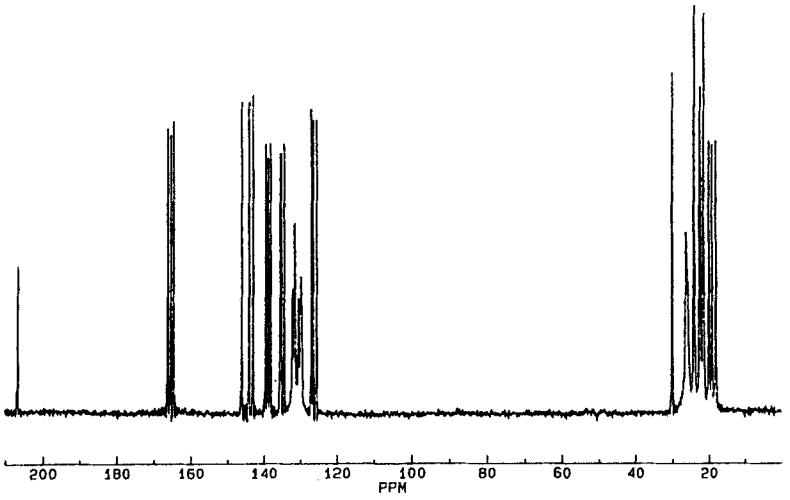

Figure 8. 45·3 MHz ^{13}C CP/MAS NMR spectrum of the TOT–acetone clathrate at room temperature. The H^1 90° pulse was 4 μs. The contact time was 3 ms and the relaxation delay was 2 s. The first-order spinning sidebands were suppressed with a pulse sequence described by Hemminga and de Jager[63]

30·1 ppm from TMS for the carbonyl and methyl carbons, respectively.

In order to confirm the ^2H NMR data, the chemical shielding tensor of the carbonyl carbon of TOT enclathrated [2-^{13}C] acetone was examined at room temperature. Previous studies[61,62] have shown that the chemical shielding parameters for the carbonyl carbon of solid acetone at 87 K are $\sigma_{xx} = -58 \pm 6$ ppm, $\sigma_{yy} = -72 \pm 6$ ppm and $\sigma_{zz} = 130 \pm 6$ ppm with respect to the isotropic chemical shift, taken to be 0 ppm. The σ_{zz} component has been shown to be perpendicular to the sp^2 molecular plane. The other two components are parallel and perpendicular to the carbonyl bond in the molecular plane. The previous studies were unable to assign the orientations to the σ_{xx} and σ_{yy} components. Methyl group rotations will leave this tensor completely unchanged. The four-site reorientational motion, on the other hand, will cause σ_{zz} and one of the other two parameters to be averaged. By observing the ^{13}C powder spectrum at room temperature it is possible to determine the orientation of σ_{xx} and σ_{yy} at 87 K, depending on which one remains unchanged at room temperature.

Initially, a static ^{13}C CP spectrum of unlabelled TOT–acetone was obtained and subtracted from a similar spectrum of TOT–[2-^{13}C] acetone. Since the enrichment of ^{13}C was only 12 mol%, the signal-to-noise ratio in the difference spectrum was too low to make a reliable measurement of the shielding parameters. Instead, ^{13}C CP/MAS spectra were obtained for the enriched sample at slow spinning rates so that the graphical sideband analysis of Herzfeld and Berger[49] could be used to obtain the chemical shielding parameters. The shielding parameters obtained from this method were $\sigma'_{xx} = -39 \pm 6$ ppm, $\sigma'_{yy} = -53 \pm 6$ ppm and $\sigma'_{zz} = 92 \pm 9$ ppm with respect to the isotropic resonance at 0 ppm. The line shapes were reconstructed[43,44] for both the pure acetone at 87 K and the enclathrated acetone at room temperature and are shown in Figure 9. It is obvious that the σ_{zz} component is averaged, and therefore the motion is confirmed to be out of the molecular plane. The σ_{xx} component remained essentially unchanged, and therefore its

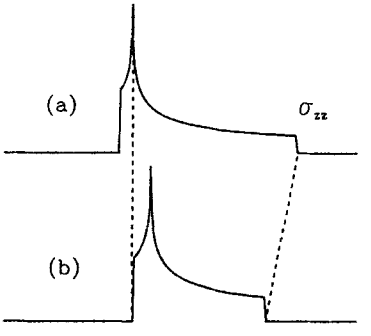

Figure 9. (a) Chemical shielding tensor powder pattern for the carbonyl carbon of solid acetone. This spectrum was reconstructed from the parameters given in the literature.[61,62] (b) The same tensor for acetone in its TOT clathrate at room temperature. This spectrum was reconstructed from the parameters obtained from the slow spinning experiments described in the text

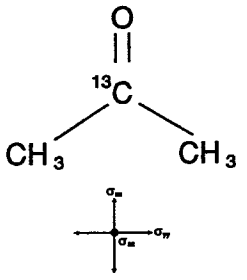

Figure 10. Orientation of the chemical shielding tensor for acetone at 87 K

orientation must be parallel to the carbonyl bond (Figure 10).

Applying the same four-site model used for the ^{2}H NMR data to the chemical shift tensors gives an analogous set of equations:

$$\sigma'_{xx} = \sigma_{zz}\frac{(1-\Omega)}{2} + \sigma_{yy}\frac{(1+\Omega)}{2} \tag{22}$$

$$\sigma'_{yy} = \sigma_{xx} \tag{23}$$

$$\sigma'_{zz} = \sigma_{zz}\frac{(1+\Omega)}{2} + \sigma_{yy}\frac{(1-\Omega)}{2} \tag{24}$$

Again, there is not a unique solution but the room temperature results are consistent, within all of the errors, with the fit of the ^{2}H NMR results. For example, one possible solution is as follows: static tensor $\sigma_{xx} = -55$ ppm, $\sigma_{yy} = -69$ ppm, $\sigma_{zz} = 124$ ppm, $\Delta E = 4{\cdot}1$ kJ mol^{-1}, $\delta = 69°$ gives an averaged tensor $\sigma'_{xx} = -42{\cdot}8$ ppm, $\sigma'_{yy} = -55{\cdot}0$ ppm, $\sigma'_{zz} = 97{\cdot}8$ ppm.

Molecular mechanics calculations

The experimentally determined crystallographic coordinates of all of the carbon and oxygen atoms of the asymmetric unit of the TOT–acetone clathrate were entered into the SYBYL[54] program. The space group symmetry elements were used to generate several unit cells. A single acetone molecule with its closest eight TOT molecules were selected and all other molecules were neglected. This represents an isolated clathrate

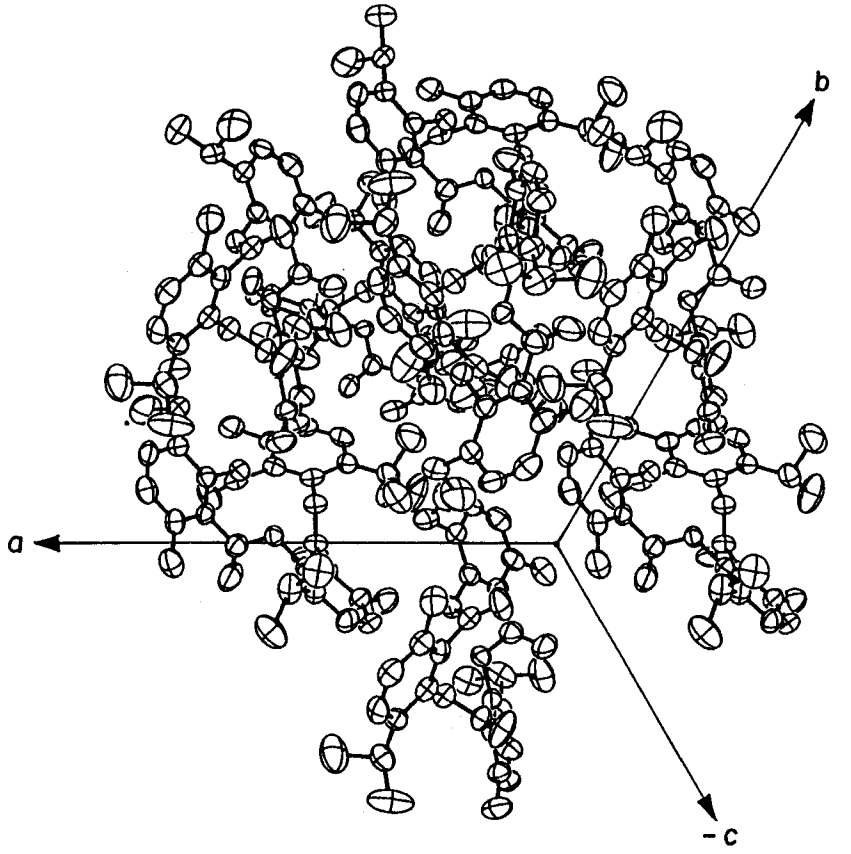

Figure 11. Depiction of the occupied TOT cage used in the molecular modelling calculations

cage with a single guest molecule and is depicted in Figure 11. The protons were generated by the program and their positions were calculated to give the entire structure a minimum energy. The positions of all of the atoms of the cage were then fixed and the enclathrated acetone molecule was rotated about its carbonyl bond in 10° steps. The relative coordinates of the methyl groups and the absolute coordinates of the sp^2 carbon and oxygen atoms of the acetone molecule were kept constant. The energy of the system was calculated for each rotational step. The energies obtained from these calculations were found to depend strongly on the O=C—C—H torsion angles of the acetone molecule, so the procedure was carried out for four different situations: $(O{=}C{-}C{-}H)_1 = (O{=}C{-}C{-}H)_2 = 0°$; $(O{=}C{-}C{-}H)_1 = 30°$, $(O{=}C{-}C{-}H)_2 = -30°$; $(O{=}C{-}C{-}H)_1 = (O{=}C{-}C{-}H)_2 = 60°$ and $(O{=}C{-}C{-}H)_1 = 0°$, $(O{=}C{-}C{-}H)_2 = 60°$. The results of the calculations are shown in Figure 12(a). Figure 12(b) is the average energy for the four situations depicted in Figure 12(a). Such an average crudely accounts for the methyl group rotation in the acetone molecule. One can see that the general shape of the potential plot is similar to that used to model the fit to the ^2H NMR data (Figure 6). Both are twofold symmetric and chiral. However, the activation barrier determined from the molecular mechanics calculations is approximately 20 times that determined from the ^2H T_1 data. The unreasonably high value may be the result of cumulative errors in the potential functions of the 410 atoms needed to model the system. Error may also result from the assumptions that the entire cage is both isolated and rigid and that the acetone molecule does not undergo any translational motion during the course of the rotation.

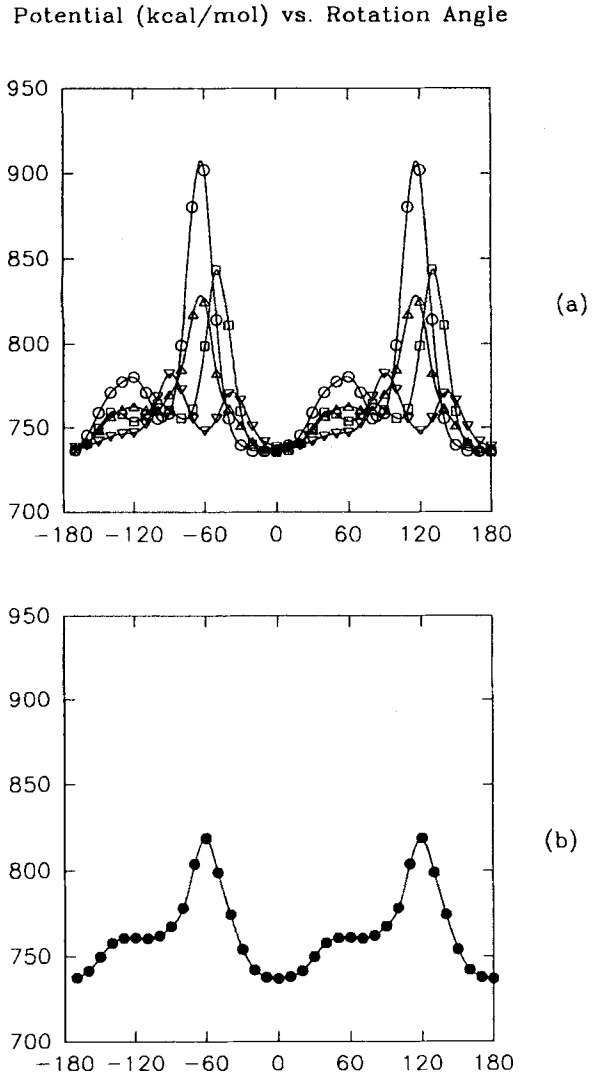

Figure 12. (a) Orientation-dependent potential for the rotation of TOT-enclathrated acetone about its carbonyl bond. ○, $(O{=}C{-}C{-}H)_1 = (O{=}C{-}C{-}H)_2 = 0°$; □, $(O{=}C{-}C{-}H)_1 = 30°$, $(O{=}C{-}C{-}H)_2 = -30°$; ▽, $(O{=}C{-}C{-}H)_1 = (O{=}C{-}C{-}H)_2 = 60°$; and △, $(O{=}C{-}C{-}H)_1 = 0°$, $(O{=}C{-}C{-}H)_2 = 60°$. (b) Mean potential from the curves in (a)

Qualitatively the calculations justify the choice of model used to analyze the ^2H NMR lineshapes. At the same time they emphasize the complexity of the system, where the dynamics of the various rotationally mobile methyl groups, on both the acetone and the TOT host, will clearly affect the overall potential. The ring methyls are generally rapid rotors on an NMR time scale at all temperatures above 77 K, whereas the isopropyl methyls can be expected to have their motional onset temperatures between 100 and 200 K. In the light of these dynamic interactions, plus the larger amplitude anisotropic thermal parameters observed for the host lattice carbonyl oxygen, it is clear that the guest–host potential has a large dynamic component, and that significant coupling between guest and host motions must be present.

CONCLUSION

Solid-state NMR, single-crystal x-ray diffraction and molecular mechanics calculations were used to obtain a very detailed description of the orientation and dynamics of TOT enclathrated acetone. Such a complete description cannot be obtained from any of these techniques individually. The x-ray data showed that the carbonyl bond of the acetone molecule was coincident with the twofold axis of the clathrate cavity and that the molecule exhibited no large-scale disorder. From both the ^2H and ^{13}C NMR results it was concluded that a number of dynamic processes were present. At tem-

peratures $\geqslant 77$ K the methyl groups of the enclathrated acetone undergo rotation at a rates $\geqslant 10^7$ Hz. Above 77 K a new slow motion sets in which is primarily a twofold flip of the acetone molecule about the carbonyl bond with an activation energy of $13{\cdot}6 \pm 0{\cdot}8$ kJ mol^{-1}. From the temperature dependence of the fast motion lineshape, it is clear that there is a secondary site energetically less favourable by $4{\cdot}4 \pm 0{\cdot}5$ kJ mol^{-1} situated $63 \pm 10^\circ$ away from the favoured site. The general shape of the potential was confirmed by using molecular modelling calculations, which proved to be remarkably sensitive to the orientation of the methyl groups. Quantitative agreement may well be difficult to achieve, as account must be taken of many dynamic H–H interactions in mobile methyl groups. However, the approximate calculations do show a twofold chiral potential. The acetone clathrate of tri-*o*-thymotide represents a simple yet challenging example of how the use of complementary techniques such as x-ray diffraction, solid-state NMR and molecular modelling can be used to define the structure and dynamics of the system. The x-ray diffraction results are needed to define the time-weighted average position of the guest in the host cavity, the NMR data are then needed to map the other low-energy positions and the time scale for motions and the modelling calculations confirm the motional model in terms of a potential calculated from the structure.

Supplementary x-ray crystal data available from the authors on request.

ACKNOWLEDGEMENT

G. Facey and J. Ripmeester are grateful for the financial support of the NSERC.

REFERENCES

1. J. Allemand and R. Gerdil, *Acta Crystallogr., Sect B* **38**, 1473 (1982).
2. J. Allemand and R. Gerbil, *Cryst Struct. Commun.* **10**, 33 (1981).
3. D. B. Boyd and K. B. Lipkowitz, *J. Chem. Educ.* **59** 269 (1982).
4. P. J. Cox, *J. Chem. Educ.* **59**, 275 (1982).
5. E. M. Engler, J. D. Andose and P. von R. Schleyer, *J. Am. Chem. Soc.* **95**, 8005 (1973).
6. N. L. Allinger, M. T. Tribble, M. A. Miller and D. H. Wertz, *J. Am. Chem. Soc.* **93**, 1637 (1971).
7. N. L. Allinger and J. T. Sprague, *J. Am. Chem. Soc.* **95**, 3893 (1973).
8. N. L. Allinger, J. T. Sprague and T. Liljefors, *J. Am. Chem. Soc.* **96**, 5100 (1974).
9. S. Fitzwater and L. S. Bartell, *J. Am. Chem. Soc.* **98**, 5107 (1976).
10. J. Kao and N. L. Allinger, *J. Am. Chem. Soc.* **99**, 975 (1977).
11. M. G. Still and L. B. Rogers, *J. Compute. Chem.* **11**, 242 (1990).
12. B. L. Podlogar and D. J. Raber, *J. Org. Chem.* **54**, 5032 (1989).
13. J. H. Lii and N. L. Allinger, *J. Am. Chem. Soc.* **111**, 8576 (1989).
14. N. L. Allinger, Y. H. Yuh and J. H. Lii, *J. Am. Chem. Soc.* **111**, 8551 (1989).
15. N. L Allinger, *J. Am. Chem. Soc.* **99**, 8126 (1977).
16. *QCPE Program No. 514 (Bigstrn-3)*, Department of Chemistry, Indiana University.
17. C. A. Venanzi, P. M. Canzius, Z. Zhang and J. D. Bunce, *J. Comput. Chem.* **10**, 1038 (1989).
18. J. H. Lii and N. L. Allinger, *J. Am. Chem. Soc.* **111**, 8566 (1989).
19. R. Däppen, H. R. Karfunkel and F. J. J. Leussen, *J. Comput. Chem.* **11**, 181 (1990).
20. W. D. Ollis and I. O. Sutherland, *J. Chem. Soc., Chem. Commun.* 402 (1966).
21. A. P. Downing, W. D. Ollis and I. O. Sutherland, *J. Chem. Soc.* 24 (1970).
22. A. C. D. Newman and H. M. Powell, *J. Chem. Soc.* 3747 (1952).
23. D. Lawton and H. M. Powell, *J. Chem. Soc.* 2339 (1958).
24. R. Gerdil, *Top. Curr. Chem.* **140**, 71 (1987).
25. D. J. Williams and D. Lawton, *Tetrahedron Lett.* 111 (1975).
26. J. Allemand and R. Gerdil, *Acta Crystallogr., Sect. C* **39**, 260 (1983).
27. R. Arad-Yellin, S. Brunie, B. S. Green, M. Knossow and G. Tsoucaris, *J. Am. Chem. Soc.* **101**, 7529 (1979).
28. R. Arad-Yellin, B. S. Green, M. Knossow and G. Tsoucaris, *Tetrahedron Lett.* **21**, 387 (1980).
29. R. Arad-Yellin, B. S. Green, M. Knossow and G. Tsoucaris, *J. Am. Chem. Soc.* **105**, 4561 (1983).
30. J. Allemand and R. Gerdil, *Acta Crystallogr., Sect. B* **38**, 2312 (1982).
31. J. Siripitayananon and R. Gerdil, *Acta Crystallogr, Sect. C* **45**, 768 (1988).
32. J. A. Ripmeester and N. E. Burlinson, *J. Am. Chem. Soc.* **107**, 3713 (1985).
33. R. Arad-Yellin, B. S. Green and M. Knossow, *J. Am. Chem. Soc.* **102**, 1157 (1980).
34. R. Gerdil, J. Allemand, and G. Bernardinelli, *Acta Crystallogr., Sect. A* **37**, C92 (1981).
35. R. Gerdil and J. Allemand, *Helv. Chim. Acta* **63**, 1750 (1980).
36. G. Facey and J. A. Ripmeester, *J. Chem. Soc., Chem. Commun.* 1585 (1990).
37. R. Bishop and I. Dance, *Top. Curr. Chem.* **149**, 161 (1988).
38. R. Arad-Yellin, B. S. Green, M. Knossow and G. Tsoucaris, in *Inclusion Compounds*, edited by J. L. Atwood, J. E. D. Davies and D. D. MacNicol, Vol. 3, Chapt. 9. Academic Press, London (1984).
39. H. W. Spiess, *Colloid Polym. Sci.* **261**, 193 (1983).
40. H. W. Spiess, *Adv. Polym. Sci.* **66**, 23 (1985).
41. J. Mathews and R. L. Walker, *Mathematical Methods of Physics*, p. 374. Benjamin, New York (1965).
42. C. I. Ratcliffe, *J. Phys. Chem.* **91**, 6464 (1987).
43. N. Bloembergen and T. S. Rowland, *Phys. Rev.* **55**, 1679 (1965).
44. N. Bloembergen and T. S. Rowland, *Acta Metall.* **1**, 731 (1953).
45. A. Abragam, in *The Principles of Nuclear Magnetism*,

edited by R. K. Adair, R. J. Elliot, W. C. Marshall and D. H. Wilkinson. Clarendon Press, Oxford (1961), Chapters 8 and 10.
46. D. A. Torchia and A. Szabo, *J. Magn. Reson.* **49**, 107 (1982).
47. M. Bloembergen, E. M. Purcell and R. V. Pound, *Phys. Rev.* **73**, 679 (1948).
48. S. Albert, H. S. Gutowsky and J. A. Ripmeester, *J. Chem. Phys.* **64**, 3277 (1976).
49. J. Herzfeld and A. E. Berger, *J. Chem. Phys.* **73**, 6021 (1980).
50. R. Spallino and G. Provenzal, *Gazz. Chim. Ital.* **39**, 325 (1909).
51. W. Baker, B. Gilbert and W. D. Ollis, *J. Chem. Soc.* 1443 (1952).
52. E. G. Gabe, Y. LePage, J. P. Charland, S. L. Lee and P. S. White, *J. Appl. Crystallogr.* **22**, 384 (1989).
53. J. H. Davis, K. R. Jeffrey, M. Bloom, M. I. Valic and T. P. Higgs, *Chem. Phys. Lett.* **42**, 390 (1976).
54. *SYBYL, Version 5.4, January 1991*. Tripos Associates, a subsidiary of Evans and Sutherland, St. Louis, MO (1991).
55. These parameters were calculated using averaged parameters given by R. G. Barnes in Ref. 56.
56. R. G. Barnes, *Adv. Nuclear Quadrupolar Reson.* **1**, 335 (1974).
57. R. G. Barnes and J. W. Bloom, *Mol. Phys.* **25**, 493 (1973).
58. T. Iijima, *Bull. Chem. Soc. Jpn.* **45**, 3526 (1972).
59. J. D. Swalen and C. C. Costain, *J. Chem. Phys.* **31**, 1562 (1959).
60. R. Nelson and L. Pierce, *J. Mol. Spectrosc.* **18**, 344 (1965).
61. A. Pines, M. G. Gibby and J. S. Waugh, *Chem. Phys. Lett.* **15**, 373 (1972).
62. W. S. Veeman, *Prog. Nucl. Magn. Reson. Spectrosc.* **16**, 193 (1983).
63. M. A. Hemminga and P. A. de Jager, *J. Magn. Reson.* **51**, 339 (1983).